
Optimal detection of the feature matching map in presence of noise and outliers

Anonymous Author(s)

Affiliation

Address

email

Abstract

2 We consider the problem of finding the matching map between two sets of d -
 3 dimensional vectors from noisy observations, where the second set contains outliers.
 4 The matching map is then an injection, which can be consistently estimated only
 5 if the vectors of the second set are well separated. The main result shows that,
 6 in the high-dimensional setting, a detection region of unknown injection may be
 7 characterized by the sets of vectors for which the inlier-inlier distance is of order
 8 at least $d^{1/4}$ and the inlier-outlier distance is of order at least $d^{1/2}$. These rates
 9 are achieved using the estimated matching minimizing the sum of logarithms of
 10 distances between matched pairs of points. We also prove lower bounds establishing
 11 optimality of these rates. Finally, we report the results of numerical experiments on
 12 both synthetic and real world data that illustrate our theoretical results and provide
 13 further insight into the properties of the estimators studied in this work.

14 1 Introduction

15 Finding the best match between two clouds of points is a problem encountered in many real problems.
 16 In computer vision, one can look for correspondences between two sets of local descriptors extracted
 17 from two images. In text analysis, one can be interested in matching vector representations of the
 18 words of two similar texts, potentially in two different languages. The goal of the present work is to
 19 gain theoretical understanding of the statistical limits of the matching problem.

20 In the sequel, we use the notation $[n] = \{1, \dots, n\}$ for any integer n , and define $\|\cdot\|$ as the Euclidean
 21 norm in \mathbb{R}^d . Assume that two independent sequences $\mathbf{X} = (X_i; i \in [n])$ and $\mathbf{Y} = (Y_i; i \in [n])$ of
 22 independent vectors are generated such that X_i and Y_i are drawn from the same distribution P_i on \mathbb{R}^d ,
 23 for every $i \in [n]$. The statistician observes the sequence \mathbf{X} and a shuffled version $\mathbf{X}^\#$ of the sequence
 24 \mathbf{Y} . More precisely, $\mathbf{X}^\#$ is such that $X_i^\# = Y_{\pi^*(i)}$ for some unobserved permutation π^* . The goal of
 25 matching is to estimate the permutation π^* from data $(\mathbf{X}, \mathbf{X}^\#)$. In the case of Gaussian distributions
 26 P_i , this problem has been studied in (Collier and Dalalyan, 2013, 2016). Clearly, consistent estimation
 27 of the matching map π^* is impossible if there are two data generating distributions P_i and P_j that are
 28 very close. In (Collier and Dalalyan, 2013, 2016), a precise quantification of the separation between
 29 these distributions is given that enables consistent estimation of π^* . Furthermore, it is shown that the
 30 permutation estimator minimizing the sum of logarithms of pairwise distances between the elements
 31 of \mathbf{X} and the elements of the shuffled version $\mathbf{X}^\#$ is an optimal estimator of π^* .

32 In this paper, we extend the model studied in (Collier and Dalalyan, 2016) to the case when the set $\mathbf{X}^\#$
 33 is contaminated by outliers. The number of outliers is supposed to be known and is equal to $m - n$,
 34 where $n = |\mathbf{X}|$ and $m = |\mathbf{X}^\#|$ are the sizes of considered two sequences, however the indices of the

	Without outliers (Collier and Dalalyan, 2016)	With outliers this paper
known $\sigma^\#$ or all equal $\sigma^\#$ s	LSNS is optimal $\bar{\kappa} \gtrsim (d \log n)^{1/4}$	LSNS is optimal [Thm. 1] $\bar{\kappa}_{\text{in-in}} \wedge \bar{\kappa}_{\text{in-out}} \gtrsim (d \log(nm))^{1/4}$
unknown $\sigma^\#$ $\sigma_{\max}/\sigma_{\min} \leq C$	LSL is optimal $\bar{\kappa} \gtrsim (d \log n)^{1/4}$	LSL is optimal [Thm. 4] $\bar{\kappa}_{\text{in-in}} \gtrsim (d \log(nm))^{1/4}$ & $\bar{\kappa}_{\text{in-out}} \gtrsim d^{1/2}$
unknown $\sigma^\#$ arbitrary		LSL is optimal [Thm. 2, 3] $\bar{\kappa}_{\text{in-in}} \wedge \bar{\kappa}_{\text{in-out}} \gtrsim d^{1/2}$

Table 1: A brief overview of the contributions in the high-dimensional regime $d \geq c \log n$. The table provides the condition on the normalized inlier-inlier distance $\bar{\kappa}_{\text{in-in}}$ and inlier-outlier distance $\bar{\kappa}_{\text{in-out}}$, making it possible to consistently detect the matching map between two sets of d -dimensional vectors. LSL and LSNS refer to least sum of logarithms and least sum of normalized squares, respectively.

outliers are unknown. All the distributions are assumed in this paper to be spherical Gaussian, although all the probabilistic tools used in the proofs have their sub-Gaussian counterparts. Thus, we consider that two spherical Gaussian distributions ¹ $P_1 = \mathcal{N}_d(\mu_1, \sigma_1^2 \mathbf{I}_d)$ and $P_2 = \mathcal{N}_d(\mu_2, \sigma_2^2 \mathbf{I}_d)$ are well separated if the “distance to noise ratio” $\kappa(P_1, P_2) = \|\mu_1 - \mu_2\| / \sqrt{\sigma_1^2 + \sigma_2^2}$ is large. Main findings of (Collier and Dalalyan, 2016), in terms of smallest separation distance $\bar{\kappa} = \min_{i \neq j} \kappa(P_i, P_j)$ are summarized in the second columns of Table 1. Likewise, the last column of the table provides a summary of the contributions of the present paper in terms of $\bar{\kappa}_{\text{in-in}} = \min_{i \neq j} \kappa(P_i, P_j)$ and $\bar{\kappa}_{\text{in-out}} = \min_{i,j} \kappa(P_i, Q_j)$, where Q_1, \dots, Q_{m-n} are the distributions of the outliers.

An unexpected finding of this work is that the “degree” of heteroscedasticity of the model has a strong impact on the separation distances and the detection regions (sets of values of $(\bar{\kappa}_{\text{in-in}}, \bar{\kappa}_{\text{in-out}})$ for which it is possible to detect the feature map π^*). This is in sharp contrast with the outlier-free case, where consistent estimation requires $\bar{\kappa}$ to be at least of order $(d \log n)^{1/4}$ irrespective of the behaviour of variances of P_i . We prove in this work that in the high dimensional regime $d \geq c \log n$, which is arguably more appealing than the low dimensional regime $d \leq c \log n$, the following statements are true:

- If there is no heteroscedasticity, *i.e.*, when all the variances are equal, consistent estimation of π^* is possible if and only if $\bar{\kappa} = \bar{\kappa}_{\text{in-in}} \wedge \bar{\kappa}_{\text{in-out}}$ is at least of order $(d \log(nm))^{1/4}$. This is the same rate as in the outlier-free case.
- If the heteroscedasticity is mild, *i.e.*, all the variances are of the same order, the condition $\bar{\kappa}_{\text{in-in}} \gtrsim (d \log(nm))^{1/4}$ is the same as in the previous item, but the stronger condition $\bar{\kappa}_{\text{in-out}} \gtrsim d^{1/2}$ is needed for the inlier-outlier separation distance.
- Finally, in the general heteroscedastic setting both $\bar{\kappa}_{\text{in-in}}$ and $\bar{\kappa}_{\text{in-out}}$ should be at least of order $d^{1/2}$. Furthermore, in all these cases consistent estimation is performed by the same estimator: the Least Sum of Logarithms (LSL).

Note also that the empirical evaluation done in this paper shows that LSL is interesting not only from the theoretical but also from the practical point of view.

Agenda Section 2 describes the framework of the vector matching problem and introduces the terminology used throughout this paper. Precise statements of the main theoretical results are gathered in Section 3. The prior work is briefly discussed in Section 4. Section 5 contains numerical experiments carried out both for synthetic and real data. A brief summary and some concluding remarks are presented in Section 6. Proofs of all theoretical claims are deferred to the supplemental material.

2 Problem Formulation

We begin with formalizing the problem of matching two sequences of feature vectors (X_1, \dots, X_n) and $(X_1^\#, \dots, X_m^\#)$ with different sizes n and m such that $m \geq n \geq 2$. In what follows, we assume

¹We use the notation \mathbf{I}_d for the $d \times d$ identity matrix

69 that the observed feature vectors are randomly generated from the model

$$\begin{cases} X_i = \theta_i + \sigma_i \xi_i, \\ X_j^\# = \theta_j^\# + \sigma_j^\# \xi_j^\#, \end{cases} \quad i = 1, \dots, n \text{ and } j = 1, \dots, m. \quad (1)$$

70 In this model, illustrated in Figure 1, it is assumed that

- 71 • $\boldsymbol{\theta} = (\theta_1, \dots, \theta_n)$ and $\boldsymbol{\theta}^\# = (\theta_1^\#, \dots, \theta_m^\#)$ are two sequences of vectors from \mathbb{R}^d , corresponding to the original features, which are unavailable,
- 72 • $\boldsymbol{\sigma} = (\sigma_1, \dots, \sigma_n)^\top$, $\boldsymbol{\sigma}^\# = (\sigma_1^\#, \dots, \sigma_m^\#)^\top$ are positive real numbers corresponding to the magnitudes of the noise contaminating each feature,
- 73 • ξ_1, \dots, ξ_n and $\xi_1^\#, \dots, \xi_m^\#$ are two independent sequences of i.i.d. random vectors drawn from the Gaussian distribution with zero mean and identity covariance matrix.

74
75
76
77 The simplest special case of (1), considered in (Collier and Dalalyan, 2016), corresponds to the situation where a perfect matching exists between the two sequences $\boldsymbol{\theta}$ and $\boldsymbol{\theta}^\#$. This means that 78 $m = n$ and, for some bijective mapping $\pi^* : [n] \rightarrow [n]$, $\theta_i = \theta_{\pi^*(i)}^\#$ for all $i \in [n]$. In the general case, 79 both $\mathbf{X} = (X_1, \dots, X_n)$ and $\mathbf{X}^\# = (X_1^\#, \dots, X_m^\#)$ may contain outliers, *i.e.* feature vectors that have no corresponding pair. In such a situation, it is merely assumed that there exists a set $S \subset [n]$ 80 and an injective mapping $\pi^* : S \rightarrow [m]$ such that

$$\theta_i = \theta_{\pi^*(i)}^\# \quad \text{and} \quad \sigma_i = \sigma_{\pi^*(i)}^\#, \quad \forall i \in S. \quad (2)$$

81
82
83 In this case we say that the vectors $\{X_i : i \in [n] \setminus S\}$ and $\{X_j^\# : j \in [m] \setminus \pi^*(S)\}$ are outliers. The ultimate goal is to estimate the feature matching map π^* .

84
85 In this work we consider the case when $S = [n]$ and $m > n$. This means that only the larger set of feature vectors, namely $\mathbf{X}^\#$, contains outliers. Let us also define the set $O_{\pi^*} \triangleq [m] \setminus \text{Im}(\pi^*)$, which 86 contains the indices of outliers and satisfies $|O_{\pi^*}| = m - n$. Naturally, the feature vectors contained in \mathbf{X} , as well as those vectors from $\mathbf{X}^\#$ that are not outliers, are called *inliers*. 87
88

89 In this formulation, the data generating distribution is defined by the parameters $\boldsymbol{\theta}^\#$, $\boldsymbol{\sigma}^\#$ and π^* . We omit the set of parameters $\boldsymbol{\theta}$ and $\boldsymbol{\sigma}$, since they are automatically identified using π^* , $\boldsymbol{\theta}^\#$ and $\boldsymbol{\sigma}^\#$ by 90 the formula $(\theta_i, \sigma_i) = (\theta_{\pi^*(i)}^\#, \sigma_{\pi^*(i)}^\#)$ for $i \in [n]$. Since our goal is to match the feature vectors, we 91 focus our attention on the problem of estimating the parameter π^* only, considering $\boldsymbol{\theta}^\#$ and $\boldsymbol{\sigma}^\#$ as nuisance parameters. In what follows, we denote by $\mathbf{P}_{\boldsymbol{\theta}^\#, \boldsymbol{\sigma}^\#, \pi^*}$ the probability distribution of the 92 sequence $(X_1, \dots, X_n, X_1^\#, \dots, X_m^\#)$ defined by (1) under condition (2) with $S = [n]$. 93
94

95 We are interested in designing estimators that have an expected error smaller than a prescribed level α under the weakest possible conditions on the nuisance parameter $\boldsymbol{\theta}^\#$ and noise level $\boldsymbol{\sigma}^\#$. Clearly, 96 the problem of matching becomes more difficult with hardly distinguishable features. To quantify 97 this phenomenon, we introduce the normalized separation distance $\bar{\kappa}_{\text{in-in}} = \bar{\kappa}_{\text{in-in}}(\boldsymbol{\theta}^\#, \boldsymbol{\sigma}^\#, \pi^*)$ and 98 the normalized outlier separation distance $\bar{\kappa}_{\text{in-out}} = \bar{\kappa}_{\text{in-out}}(\boldsymbol{\theta}^\#, \boldsymbol{\sigma}^\#, \pi^*)$, which measure the minimal 99 distance-to-noise ratio between inliers and the minimal distance-to-noise ratio between inliers and 100 outliers, respectively. The precise definitions read as

$$\bar{\kappa}_{\text{in-in}} \triangleq \min_{\substack{i, j \notin O_{\pi^*}, \\ j \neq i}} \frac{\|\theta_i^\# - \theta_j^\#\|}{(\sigma_i^{\#2} + \sigma_j^{\#2})^{1/2}}, \quad \bar{\kappa}_{\text{in-out}} \triangleq \min_{\substack{i \notin O_{\pi^*}, \\ j \in O_{\pi^*}}} \frac{\|\theta_i^\# - \theta_j^\#\|}{(\sigma_i^{\#2} + \sigma_j^{\#2})^{1/2}}. \quad (3)$$

101
102 Notice that $\bar{\kappa}_{\text{in-in}}$ can be rewritten as

$$\bar{\kappa}_{\text{in-in}} = \min_{\substack{i, j \in [n] \\ i \neq j}} \frac{\|\theta_i - \theta_j\|}{(\sigma_i^2 + \sigma_j^2)^{1/2}}.$$

103 Clearly, if $\bar{\kappa}_{\text{in-in}} = 0$ or, $\bar{\kappa}_{\text{in-out}} = 0$, there are two identical feature vectors in $\mathbf{X}^\#$. In such a 104 situation, assuming σ_i 's are all equal, the parameter π^* is nonidentifiable, in the sense that there 105 exist two different permutations π_1^* and π_2^* such that the distributions $\mathbf{P}_{\boldsymbol{\theta}^\#, \boldsymbol{\sigma}^\#, \pi_1^*}$ and $\mathbf{P}_{\boldsymbol{\theta}^\#, \boldsymbol{\sigma}^\#, \pi_2^*}$ 106 coincide. Therefore, to ensure the existence of consistent estimators of π^* it is necessary to impose 107 the conditions $\bar{\kappa}_{\text{in-in}} > 0$ and $\bar{\kappa}_{\text{in-out}} > 0$. Moreover, good estimators are those consistently estimating 108 π^* even if either $\bar{\kappa}_{\text{in-in}}$ or $\bar{\kappa}_{\text{in-out}}$ are small. We are interested here in finding the detection boundary in 109 terms of the order of magnitude of $(\bar{\kappa}_{\text{in-in}}, \bar{\kappa}_{\text{in-out}})$. More precisely, for any given $\alpha \in (0, 1)$ we wish 110 to find a region $\mathcal{R}_{n, m, d}^\alpha$ in \mathbb{R}^2 such that:

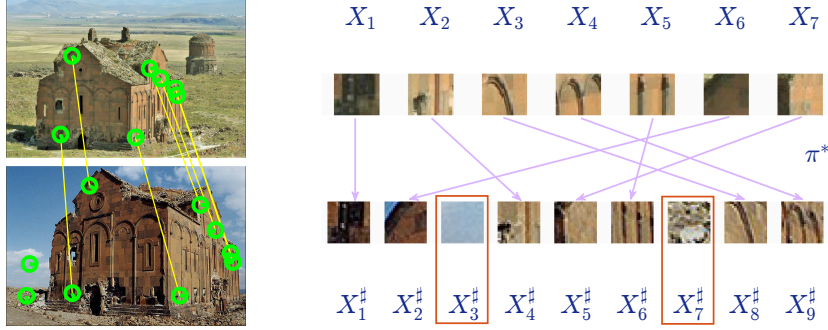


Figure 1: Illustration of the considered framework described in (1). We wish to match a set of 7 patches extracted from the first image to the 9 patches from the second image. The picture on the left shows the locations of patches as well as the true matching map π^* (the yellow lines).

- 111 • There is an estimator $\hat{\pi}_{n,m}$ of π^* satisfying $\mathbf{P}_{\theta^\#, \sigma^\#, \pi^*}(\hat{\pi} \neq \pi^*) \leq \alpha$ for every $(\theta^\#, \sigma^\#, \pi^*)$
- 112 lying in the detection region, *i.e.*, for which $(\bar{\kappa}_{\text{in-in}}, \bar{\kappa}_{\text{in-out}}) \in \mathcal{R}_{n,m,d}^\alpha$.
- 113 • There is a constant $C < 1$ such that for any estimator $\bar{\pi}_{n,m}$ of π^* , we can find a parameter value
- 114 $(\theta^\#, \sigma^\#, \pi^*)$ in the region $\{(\theta^\#, \sigma^\#, \pi^*) : (\bar{\kappa}_{\text{in-in}}, \bar{\kappa}_{\text{in-out}}) \in C\mathcal{R}_{n,m,d}^\alpha\}$ such that $\bar{\pi}$ fails to detect
- 115 π^* with a probability larger than α .

116 Let us make two remarks. First, note that in the outlier-free case considered in (Collier and Dalalyan,

117 2016), $\bar{\kappa}_{\text{in-out}}$ is meaningless and, therefore, the detection region is one-dimensional $\mathcal{R}_{n,m,d}^\alpha$. Thus,

118 it is necessarily a half-line and is proven to be of the form $\bar{\kappa}_{\text{in-in}} \geq C(\log n/\alpha)^{1/2} \vee (d \log n/\alpha)^{1/4}$

119 for some universal constant C . Second, the aforementioned definition of the detection region

120 $\mathcal{R}_{n,m,d}^\alpha$ does not guarantee its uniqueness (even up to a scaling by a universal constant). This is

121 in contrast with the outlier-free case. To overcome this difficulty, we look for $\mathcal{R}_{n,m,d}^\alpha$ of the form

122 $[t_{\text{in-in}}, +\infty) \times [t_{\text{in-out}}, +\infty)$ with the smallest possible threshold $t_{\text{in-out}}$ for the normalized inlier-outlier

123 distance $\bar{\kappa}_{\text{in-out}}$.

124 3 Main theoretical results

125 In this section, we have collected the main theoretical findings of the paper. When the noise is

126 homoscedastic, *i.e.*, when all σ 's are equal, the results obtained by Collier and Dalalyan (2016) in

127 the outlier-free setting can be easily extended to the setting with outliers. Therefore, in the present

128 paper, we focus on the heteroscedastic case. For the sake of clarity of exposition, we will present

129 the results in the case of known variances $\sigma, \sigma^\#$ prior to investigating the more interesting case of

130 unknown variances.

131 The detection regions we study below are based on the profile maximum likelihood estimator. The

132 model presented in (1) has the parameter $\Xi = (\theta^\#, \sigma^\#, \pi)$, while the observations are the sequences

133 of feature vectors \mathbf{X} and $\mathbf{X}^\#$. The negative log-likelihood of this model is given by

$$\ell_n(\Xi; \{\mathbf{X}, \mathbf{X}^\#\}) = \sum_{i=1}^n \left(\frac{\|X_i - \theta_{\pi(i)}^\#\|_2^2}{2\sigma_{\pi(i)}^{\#2}} + \frac{1}{2} \log(\sigma_{\pi(i)}^{\#2}) \right) + \sum_{j=1}^m \left(\frac{\|X_j^\# - \theta_j^\#\|_2^2}{2\sigma_j^{\#2}} + \frac{1}{2} \log(\sigma_j^{\#2}) \right).$$

134 The profile negative log-likelihood is then defined as the minimum with respect to $(\theta^\#, \sigma^\#)$ of the

135 log-likelihood $\ell_n(\Xi; \{\mathbf{X}, \mathbf{X}^\#\})$.

136 3.1 Warming up: known variances $\sigma, \sigma^\#$

137 One can check that the minimization with respect to $\theta^\#$ leads to the variance-dependent cost function

$$\ell_n(\pi, \sigma^\#; \{\mathbf{X}, \mathbf{X}^\#\}) = \sum_{i=1}^n \frac{\|X_i - X_{\pi(i)}^\#\|_2^2}{\sigma_i^2 + \sigma_{\pi(i)}^{\#2}} + \sum_{i=1}^n \frac{1}{2} \log(\sigma_{\pi(i)}^{\#2}) + \sum_{j=1}^m \frac{1}{2} \log(\sigma_j^{\#2}). \quad (4)$$

138 When $m = n$ and there is no outlier, the last two sums of the last display do not depend on π

139 and, therefore, the maximum profile likelihood estimator of π^* is obtained by the Least Sum of

140 Normalized Squares (LSNS) criterion

$$\hat{\pi}_{n,m}^{\text{LSNS}} \in \arg \min_{\pi} \sum_{i=1}^n \frac{\|X_i - X_{\pi(i)}^{\#}\|^2}{\sigma_i^2 + \sigma_{\pi(i)}^{\#}}, \quad (5)$$

141 where the minimum is over all injective mappings $\pi : [n] \rightarrow [m]$. This, and the other estimators
 142 defined in this work, can be efficiently computed using suitable versions of the Hungarian algorithm
 143 (Kuhn, 1955, 2010; Munkres, 1957). As shows the next theorem, it turns out that even when $m > n$,
 144 the estimator $\hat{\pi}_{n,m}^{\text{LSNS}}$ defined above leads to an optimal detection region.

145 **Theorem 1 (Upper bound for LSNS)** *Let $\alpha \in (0, 1)$ and condition (2) be fulfilled. If the separation*
 146 *distances $\bar{\kappa}_{\text{in-in}}$ and $\bar{\kappa}_{\text{in-out}}$ corresponding to $(\theta^{\#}, \sigma^{\#}, \pi^*)$ and defined in (3) satisfy the condition*

$$\min\{\bar{\kappa}_{\text{in-in}}, \bar{\kappa}_{\text{in-out}}\} \geq 4 \left\{ (d \log(4nm/\alpha))^{1/4} \vee (2 \log(8nm/\alpha))^{1/2} \right\} \quad (6)$$

147 *then the LSNS estimator defined in (5) detects the true matching map π^* with probability at least*
 148 *$1 - \alpha$, that is*

$$\mathbf{P}_{\theta^{\#}, \sigma^{\#}, \pi^*}(\hat{\pi}_{n,m}^{\text{LSNS}} = \pi^*) \geq 1 - \alpha.$$

149 The similarity—both its statement and its proof— of this result is to its counterpart in the outlier-free
 150 setting might suggest that the presence of outliers does not make the problem any harder from a
 151 statistical point of view. However, this is not true in the more appealing setting of unknown variances.
 152

153 3.2 Detection of π^* for unknown and arbitrary variances $\sigma, \sigma^{\#}$

154 The LSNS procedure analyzed in Theorem 1 exploits the values of known noise variances to normalize
 155 the squares of distances between vectors X_i and $X_{\pi(i)}^{\#}$. Therefore, LSNS is inapplicable in the case
 156 of unknown noise variances. Instead, we consider the Least Sum of Logarithms (LSL) estimator

$$\hat{\pi}_{n,m}^{\text{LSL}} \triangleq \arg \min_{\pi: [n] \rightarrow [m]} \sum_{i=1}^n \log \|X_i - X_{\pi(i)}^{\#}\|^2, \quad (7)$$

157 where the minimum is over all injective maps $\pi : [n] \rightarrow [m]$. This estimator can be seen as the
 158 minimizer of a criterion defined as the minimum of the cost function from (4) with respect to $\sigma^{\#}$
 159 under the constraint $\min_{j \notin \text{Im}(\pi)} \sigma_j^{\#} \geq \sigma_{\min}$, for some fixed (but unknown) constant $\sigma_{\min} > 0$.

160 To provide a quick overview of what follows, let us stick in the remaining of this paragraph to the
 161 case $\log(nm) = O(d)$ so that the right hand side of (6) is of order $(d \log(nm))^{1/4}$. Recall that in the
 162 outlier-free case, the LSL estimator has been shown to perform as well as the LSNS while having the
 163 advantage of not requiring the knowledge of variances $\sigma^{\#}$ (Collier and Dalalyan, 2016). Somewhat
 164 unexpectedly, the situation is significantly different in the presence of outliers. Indeed, the best we
 165 manage to prove in the presence of outliers is that the detection of the matching map by LSL is
 166 possible whenever $\min\{\bar{\kappa}_{\text{in-in}}, \bar{\kappa}_{\text{in-out}}\} \geq C\sqrt{d}$ for some sufficiently large constant C . The precise
 167 statement being given in the next theorem, let us mention right away that the discrepancy between
 168 this rate \sqrt{d} and the rate $(d \log(nm))^{1/4}$ in (6) is due to the inherent hardness of the setting and not
 169 merely an artefact of the proof. This will be made clear below.

170 **Theorem 2 (Upper bound for LSL)** *Let $\alpha \in (0, 1/2)$ and condition (2) be fulfilled. If the separation*
 171 *distances $\bar{\kappa}_{\text{in-in}}$ and $\bar{\kappa}_{\text{in-out}}$ corresponding to $(\theta^{\#}, \sigma^{\#}, \pi^*)$ and defined by (3) satisfy*

$$\min\{\bar{\kappa}_{\text{in-in}}, \bar{\kappa}_{\text{in-out}}\} \geq \sqrt{2d} + 4 \left\{ (2d \log(4nm/\alpha))^{1/4} \vee (3 \log(8nm/\alpha))^{1/2} \right\} \quad (8)$$

172 *then the LSL estimator (7) detects the matching map π^* with probability at least $1 - \alpha$, that is*

$$\mathbf{P}_{\theta^{\#}, \sigma^{\#}, \pi^*}(\hat{\pi}_{n,m}^{\text{LSL}} = \pi^*) \geq 1 - \alpha.$$

173 This result is disappointing since it requires the distance between different feature vectors to be larger
 174 than $\sqrt{2d}$ in order to be able to consistently estimate the matching map π^* . As we show below,
 175 without any further condition (for instance, on the noise variances), this rate cannot be improved.
 176

177 Furthermore, the rate \sqrt{d} is optimal not only for LSL but also for the larger class of so called *distance*
 178 *based M-estimators*.

179 We will say that an estimator $\hat{\pi}_n$ of π^* is a distance based *M-estimator*, if for a sequence of non-
 180 decreasing functions $\rho_i : \mathbb{R}_+ \rightarrow \mathbb{R}$, $i = 1, \dots, n$, the following is correct

$$\hat{\pi}_n \in \arg \min_{\pi: [n] \rightarrow [m]} \sum_{i=1}^n \rho_i(\|X_i - X_{\pi(i)}^\#\|),$$

181 where the minimum is over all injective mappings $\pi : [n] \rightarrow [m]$. We denote by \mathcal{M} the set of all
 182 distance based *M-estimators*. We show that there is indeed a setup where $\bar{\kappa}_{\text{in-in}} \wedge \bar{\kappa}_{\text{in-out}}$ is as large as
 183 $0.2\sqrt{d}$ but any estimator from \mathcal{M} fails to detect π^* with probability at least $1/4$. The next theorem
 184 formalizes the described result.

185 **Theorem 3 (Lower bound)** *Assume that $m > n \geq 4$ and $d \geq 422 \log(4n)$. There exists a triplet*
 186 *$(\sigma^\#, \theta^\#, \pi^*)$ such that $\bar{\kappa}_{\text{in-in}} = \bar{\kappa}_{\text{in-out}} = \sqrt{d/20}$ and*

$$\inf_{\hat{\pi} \in \mathcal{M}} \mathbf{P}_{\theta^\#, \sigma^\#, \pi^*}(\hat{\pi} \neq \pi^*) > 1/4. \quad (9)$$

187 The proof of this theorem, postponed to the appendix, is constructive. This means that we exhibit
 188 a triplet $(\sigma^\#, \theta^\#, \pi^*)$ satisfying (9). Careful inspection shows that in the case $d = O(\log(nm))$
 189 the same triplet satisfies $\bar{\kappa}_{\text{in-in}} \wedge \bar{\kappa}_{\text{in-out}} \asymp \sqrt{\log(nm)}$ and (9) is still true. This implies that the
 190 order of magnitude of the right hand side of (8) is optimal both in the high-dimensional regime
 191 $d \geq 422 \log(4n)$ and in the low-dimensional regime $d < 422 \log(4n)$. This shows the optimality of
 192 LSL among all estimators from \mathcal{M} . Note that the estimator $\hat{\pi}_{n,m}^{\text{LSNS}}$ does not belong to the family of
 193 *distance based M-estimators*. Furthermore, in the low dimensional regime $d = O(\log(nm))$, the
 194 separation rate of the LSL, $\sqrt{\log(nm)}$, is the same as that of the LSNS.
 195

196 In the next section we show that under some mild conditions on $\sigma^\#$ it is indeed possible to obtain
 197 different rates for $\bar{\kappa}_{\text{in-in}}$ and $\bar{\kappa}_{\text{in-out}}$, namely we show that if $\bar{\kappa}_{\text{in-in}} \gtrsim d^{1/4}$ and $\bar{\kappa}_{\text{in-out}} \gtrsim d^{1/2}$ then the
 198 LSL estimator detects correct matching with high probability.

199 3.3 Detection of π^* for unknown and mildly varying variances $\sigma, \sigma^\#$

200 The results of the last two theorems are disappointing, since they indicate that the features should
 201 be very different from one another for detection of the matching map to be possible. An interesting
 202 finding, presented below, is that strong constraint can be significantly alleviated in the context of mild
 203 heteroscedasticity. By mild heteroscedasticity we understand here the situation in which all variances
 204 $\sigma_i^\#$ are of the same order of magnitude.

205 **Theorem 4 (Upper bound under mild heteroscedasticity)** *Let $r_\sigma = \max_{i,j}(\sigma_i^\#/\sigma_j^\#) < \infty$. If the*
 206 *separation distances $\bar{\kappa}_{\text{in-in}}$ and $\bar{\kappa}_{\text{in-out}}$ defined in (3) satisfy*

$$\begin{aligned} \bar{\kappa}_{\text{in-in}} &\geq 2(4d \log(4nm/\alpha))^{1/4} + 2(2 \log(4nm/\alpha))^{1/2} \\ \bar{\kappa}_{\text{in-out}} &\geq \sqrt{2(r_\sigma - 1)d} + 2(4r_\sigma^2 d \log(4nm/\alpha))^{1/4} + 2(2r_\sigma \log(4nm/\alpha))^{1/2}, \end{aligned}$$

207 *then the LSL estimator (7) detects the matching map π^* with probability at least $1 - \alpha$, that is*

$$\mathbf{P}_{\theta^\#, \sigma^\#, \pi^*}(\hat{\pi}_{n,m}^{\text{LSL}} = \pi^*) \geq 1 - \alpha.$$

208 Note that a lower bound similar to that of Theorem 3 can be proved in the case of mild heteroscedasticity
 209 as well, showing that there is an example for which $\bar{\kappa}_{\text{in-in}}$ is of order $d^{1/4}$, $\bar{\kappa}_{\text{in-out}}$ is of order $d^{1/2}$
 210 and any estimator from \mathcal{M} fails to detect π^* with probability at least $1/4$.
 211

212 We complete this section by summarizing the joint contribution of Theorems 1 to 4. To simplify this
 213 discussion, we consider two cases: high-dimensional case refers to $d \geq \log(4nm/\alpha)$ (presented in
 214 Table 1) and low-dimensional case refers to the condition $d < \log(4nm/\alpha)$. In the high dimensional
 215 setting with arbitrary noise variances, the detection region for the LSL estimator is given by $\{\bar{\kappa}_{\text{in-in}} \wedge$
 216 $\bar{\kappa}_{\text{in-out}} \geq 15\sqrt{d}\}$, which is much worse than the detection region for LSNS, $\{\bar{\kappa}_{\text{in-in}} \wedge \bar{\kappa}_{\text{in-out}} \geq$
 217 $8(d \log(4nm/\alpha))^{1/4}\}$, obtained in the known-variance scenario. Somewhat surprisingly, in such a

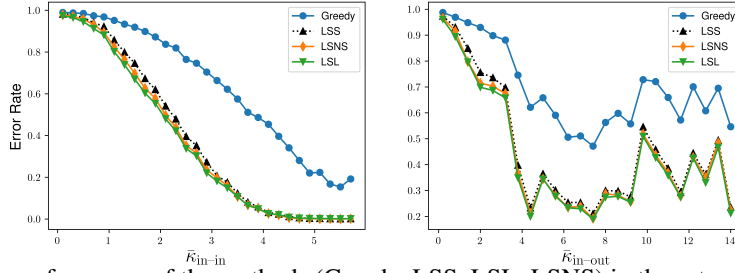


Figure 2: The performance of the methods (Greedy, LSS, LSL, LSNS) in the setup described in Exp. 1. Plots show the error rate (percentage of repetitions in which the estimated matching map differs from the true one) as a function of separation distances. The left plot illustrates that LSS, LSL and LSNS require much lower value of $\bar{\kappa}_{in-in}$ in order to find the correct mapping. The left plot shows that there is a clear improvement of the error when the inlier-inlier separation distance increases, while the right plot shows that the error rate might not be made small by augmenting $\bar{\kappa}_{in-out}$ only.

218 setting, even a strong assumption on the outliers, such as requiring them to be at least at a distance
 219 $0.2\sqrt{d}$ of the inliers, is not enough for relaxing the assumption on the inlier-inlier separation distance.
 220 Finally, on a positive note, in the intermediate case of mildly varying variances, the detection region
 221 for the LSL estimator is of the form $\{\bar{\kappa}_{in-in} \geq 7(d \log(4nm/\alpha))^{1/4}; \bar{\kappa}_{in-out} \geq 10\sqrt{d}\}$. This means
 222 that if the outliers are at a distance $\Omega(\sqrt{d})$ of the inliers, then the LSL recovers the true matching
 223 under the same condition on $\bar{\kappa}_{in-in}$ as in the outlier-free setting.

224 4 Other related work

225 Measuring the quality of the various statistical procedures of decision making by their minimal
 226 separation rates became the standard in hypotheses testing, see the seminal papers (Burnashev, 1979;
 227 Ingster, 1982) and the monographs (Ingster and Suslina, 2003; Juditsky and Nemirovski, 2020).
 228 Currently this approach is widely adopted in machine learning literature (Xing et al., 2020; Wolfer
 229 and Kontorovich, 2020; Blanchard et al., 2018; Ramdas et al., 2016; Wei et al., 2019; Collier, 2012).
 230 Beyond the classical setting of two hypotheses, it can also be applied to multiple hypotheses testing
 231 framework, for instance, variable selection (Ndaoud and Tsybakov, 2020; Azaïs and de Castro, 2020;
 232 Comminges and Dalalyan, 2012) or the matching problem considered here.

233 On the other hand, feature matching is a well studied problem in computer vision. In recent years,
 234 a great deal of attention was devoted to the acceleration of greedy matching algorithms, based on
 235 approximate and fast methods of finding nearest neighbors (e.g. Jiang et al. (2016); Wang et al.
 236 (2018); Wang (2011); Harwood and Drummond (2016); Malkov and Yashunin (2020)). Another
 237 direction that helps to improve feature matching problem is using alternative local descriptors (Rublee
 238 et al., 2011; Chen et al., 2010; Calonder et al., 2010) for given keypoints. Naturally, the question of
 239 how to chose keypoints arises, which is addressed, for instance, in (Bai et al., 2020; Tian et al., 2020).
 240 For more complete overview of the field we refer to (Ma et al., 2021) and references therein.

241 Finally, permutation estimation and related problems have been recently investigated in different
 242 contexts such as statistical seriation (Flammarion et al., 2019), noisy sorting (Mao et al., 2018),
 243 regression with shuffled data (Pananjady et al., 2017; Slawski and Ben-David, 2019), isotonic
 244 regression and matrices (Mao et al., 2020; Pananjady and Samworth, 2020; Ma et al., 2020), crowd
 245 labeling (Shah et al., 2021), and recovery of general discrete structure (Gao and Zhang, 2019).

246 5 Numerical results

247 In this section, we report the results of some numerical experiments carried out on simulated and real
 248 data. We applied aforementioned methods LSNS and LSL and computed different measures of their
 249 performance. To get a more complete picture, we included in this study the Least Sum of Squeres
 250 (LSS) estimator and the greedy estimator. LSS is an unnormalized version of LSNS, given by

$$\hat{\pi}_{n,m}^{\text{LSS}} \in \arg \min_{\pi} \sum_{i=1}^n \|X_i - X_{\pi(i)}^{\#}\|^2. \quad (10)$$

251 It coincides with LSNS in the case of homoscedastic noise. The greedy estimator is obtained
 252 by sequentially matching each vector from \mathbf{X} to the nearest vector from $\mathbf{X}^\#$. Experiments were
 253 implemented using python or matlab. For solving linear sum assignment problems such as (7) or (10),
 254 the generalized and improved versions of the Hungarian algorithm were used (Kuhn, 1955, 2010;
 255 Munkres, 1957; Duff and Koster, 2001), implemented in SciPy library (Virtanen et al., 2020).

256 **Experiment 1: Synthetic data with random features** We first randomly generated π^* , $\theta^\#$ and
 257 $\sigma^\#$ as follows. We randomly sampled from uniform distribution on $[0, 2]$ independent variables τ_{ij} ,
 258 $i \in [m]$, $j \in [d]$. Then, $(\theta_i^\#)_j$ are independently sampled from the Gaussian distribution with 0 mean
 259 and variance τ_{ij} . Additionally, for every $\theta_i^\# \in \theta^\#$ such that $i \notin J_{\pi^*}$ ($\theta_i^\#$ is an outlier), we incremented
 260 every coordinate of $\theta_i^\#$ by i . Entries of $\sigma^\#$ were sampled from the uniform distribution over $[0.5, 2]$.
 261 Sequences \mathbf{X} and $\mathbf{X}^\#$ were generated according to Section 2 with $\pi^*(i) = i$ for $i \in [n]$. We applied
 262 to this data the following matching algorithms: Greedy, LSS, LSNS and LSL.

263 We chose $n = 100$, $m = 130$ and $d = 50$, and generated $N = 50$ datasets according to the foregoing
 264 process. For each dataset, we computed the 0-1 error of the considered estimators and the values
 265 of $(\bar{\kappa}_{\text{in-in}}, \bar{\kappa}_{\text{in-out}})$. We plotted in the left (resp., the right) panel of Figure 2 the error averaged over
 266 all datasets with a given value of $\bar{\kappa}_{\text{in-in}}$ (resp. $\bar{\kappa}_{\text{in-out}}$). In this specific example, we see that the error
 267 decreases fast with $\bar{\kappa}_{\text{in-in}}$, while there is no monotonicity of the error rate as a function of $\bar{\kappa}_{\text{in-out}}$.

268 **Experiment 2: Synthetic data with deterministic features** The second experiment is conducted
 269 on data generated by features $\theta^\#$ and variances $\sigma^\#$ inspired by the example constructed in the proof
 270 of Theorem 3. More precisely, for some real numbers a and b representing, respectively, the scale of
 271 inlier-inlier distance $\bar{\kappa}_{\text{in-in}}$ and inlier-outlier distance $\bar{\kappa}_{\text{in-out}}$, we set $\theta_k^\# = [ka, 0, \dots, 0]^\top$ for $k \in [n]$
 272 and $\theta_{n+k}^\# = [na + kb, 0, \dots, 0]^\top$. We also used decreasing variances $\sigma_k^\# = 1/k^{3/2}$ for $k \in [m]$ and
 273 true identity mapping $\pi^*(k) = k$ for $k \in [n]$. We chose $n = 100$, $m = 120$ and dimension d varying
 274 in the set $\{10, 20, 40\}$. For each pair of values (a, b) in a suitably chosen grid, we repeated $n_{\text{rep}} = 400$
 275 times the experiment that consisted in generating data according to (1) and computing estimators
 276 $\hat{\pi}_{n,m}^{\text{LSS}}$ and $\hat{\pi}_{n,m}^{\text{LSL}}$ defined respectively by (10) and (7). We then computed, for each pair (a, b) and for
 277 each estimator LSS and LSL, the percentage of successful detection among n_{rep} repetitions.

278 The obtained detection regions are depicted in Figure 3 in the form of heatmaps. This visualisation
 279 allows us to grasp the forms of the detection regions for the specific choice of parameters considered
 280 in this example. The first observation is that LSL is clearly superior to LSS for all the considered
 281 values of the dimension. Second, we clearly see the deterioration of the detection region when the
 282 dimension d becomes larger. Third, the values of $\bar{\kappa}_{\text{in-out}}$ used in the plots are at least one order of
 283 magnitude larger than those of $\bar{\kappa}_{\text{in-in}}$. This is in line with the claim of Theorem 4. We also observe in
 284 these pictures that successful detection occurs when $\bar{\kappa}_{\text{in-out}}$ is larger than some threshold even if $\bar{\kappa}_{\text{in-in}}$
 285 is small. This must be a nice feature of LSL and LSS in this specific example, which unfortunately
 286 does not generalize to other examples as shown by our theoretical results.

287 **Experiment 3: Real data example** This experiment is conducted on the IMC-PT 2020 dataset
 288 from Jin et al. (2020) that consists of images of 16 different scenes with corresponding 3D point-
 289 clouds of landmarks, which are used to obtain (pseudo) ground-truth local keypoint matchings. For a
 290 given scene, we sampled 1000 pairs of distinct images of the same landmark with different camera
 291 locations, angles, weather conditions etc. For each image pair we generated 2D keypoints from
 292 original set of 3D points (note that the same 3D point appears in both of the images, so we have
 293 ground truth keypoint matching between 2 images). Subsequently, we computed SIFT descriptors
 294 (Lowe, 2004) for every keypoint in images using Python OpenCV interface (Itseez, 2015). Some
 295 pairs of images being more challenging than others, we split the dataset into two sets of image pairs in
 296 order to gain more understanding on the behaviour of the algorithms. The challenging pairs are those
 297 for which the OpenCV default matching algorithm has accuracy less than 0.5. Then, for every image
 298 pair, we fixed randomly chosen 100 keypoints in the first image (and corresponding keypoints in the
 299 second image) and added outliers to the second image from the remaining keypoints. The outlier
 300 rate is chosen to be between 0% to 70%. Finally, 3 descriptor matching algorithms were applied
 301 (OpenCV default matching algorithm, LSS and LSL). Note that σ and $\sigma^\#$ from (1) are unknown,
 302 hence LSNS is not applicable. One can consider using the estimates $\hat{\sigma}$ and $\hat{\sigma}^\#$ instead of σ and $\sigma^\#$
 303 in (5), but this is beyond the scope of this paper. Further details on this experiment along with some
 304 additional results are deferred to the supplemental material (Appendix D).

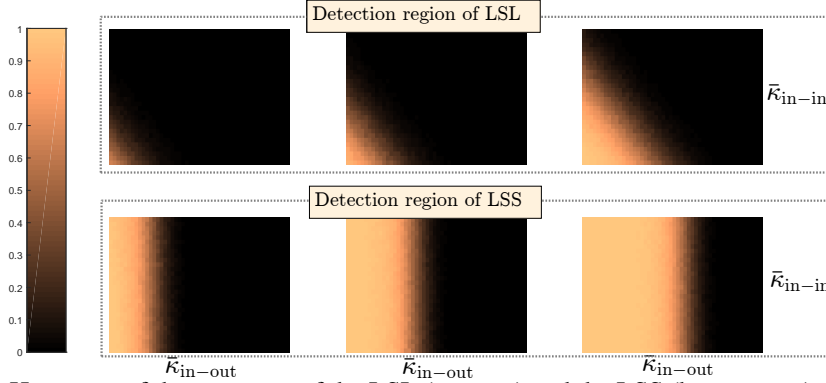


Figure 3: Heatmaps of the error rate of the LSL (top row) and the LSS (bottom row) estimators in Experiment 2. We chose $n = 100$, $m = 120$ and $d \in \{10, 20, 40\}$ from left to right. The parameter a representing the scale of $\bar{\kappa}_{\text{in-in}}$ and corresponding to y -axis varies from 0.02 to 0.08, whereas b representing the scale of $\bar{\kappa}_{\text{in-out}}$ and corresponding to x -axis varies from 0.3 to 10. Dark colour means that probability of successful detection is close to 1 (error rate close to zero).

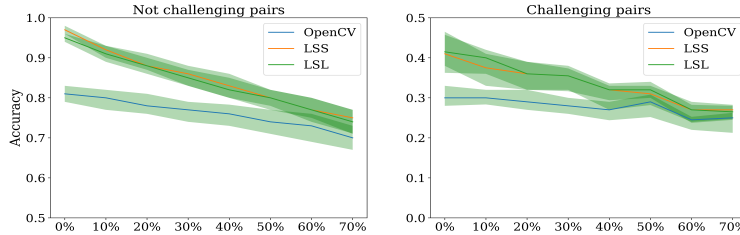


Figure 4: The estimation accuracy measured in the Hamming loss of the estimated matching in Exp. 3 for different values of the outlier rate, $(m-n)/n$, varying from 0% to 70%. The medians of estimation accuracy both for challenging pairs (right plot) and simple pairs (left plot) of images from Temple Nara scene was computed using OpenCV, LSS and LSL matchers. The green region represents the interquartile range (lower and upper bounds being 25% and 75% percentiles, respectively).

305 The median estimation accuracy measured in the Hamming loss—for the image pairs from Temple
 306 Nara Japan scene—is plotted in Figure 4. Similar results for other scenes are presented in the
 307 supplemental material. The error bars with borderlines corresponding to 75% and 25% percentiles
 308 are also displayed. The first observation is that LSS and LSL outperform the OpenCV matcher in
 309 terms of Hamming distance. Second, the task of feature matching becomes harder with the growth
 310 of outlier rate, with a deterioration that seems to be linear in the rate of outliers. Notice that in this
 311 experiment the outliers can be very similar to the inliers and the separation condition imposed on
 312 $\bar{\kappa}_{\text{in-out}}$, of Theorems 2 and 4, is violated. This implies that the larger the outlier rate the harder it is to
 313 find the correct match, causing a larger number of mistakes.

314 6 Conclusion

315 We have investigated the detection regions in the problem of estimation of the matching map between
 316 two sequences of noisy vectors. We have shown that the presence of outliers in one of the two
 317 sequences has a strong negative impact on the detection region. Interestingly, this negative impact is
 318 mitigated in the regime of mild heteroscedasticity, *i.e.*, when noise variances are of the same order
 319 of magnitude. In the extremely favorable case of homoscedastic noise (all variances are equal), the
 320 presence of outliers does not make the problem any harder, provided that the outliers are at least as
 321 different from inliers as two distinct inliers are different one another. Precise forms of the detection
 322 region in these different cases can be found in Table 1. The results of the numerical experiments
 323 conducted on both synthetic and real data confirm our findings and, furthermore, show the good
 324 behaviour of the LSL estimator in terms of its robustness to noise and to outliers, not only in the
 325 problem of detection but also in the problem of estimation. In the future, we plan to investigate the
 326 case when both sequences contain outliers and to obtain theoretical guarantees on the estimation error
 327 measured by the Hamming distance.

References

- 328
- 329 Azais, J. M. and de Castro, Y. (2020). Multiple testing and variable selection along least angle
330 regression’s path.
- 331 Bai, X., Luo, Z., Zhou, L., Fu, H., Quan, L., and Tai, C.-L. (2020). D3feat: Joint learning of dense
332 detection and description of 3d local features. In *Proceedings of the IEEE/CVF Conference on
333 Computer Vision and Pattern Recognition (CVPR)*.
- 334 Blanchard, G., Carpentier, A., and Gutzeit, M. (2018). Minimax Euclidean separation rates for testing
335 convex hypotheses in \mathbb{R}^d . *Electron. J. Stat.*, 12(2):3713–3735.
- 336 Burnashev, M. V. (1979). On the minimax detection of an inaccurately known signal in a white
337 Gaussian noise background. *Theory Probab. Appl.*, 24:107–119.
- 338 Calonder, M., Lepetit, V., Strecha, C., and Fua, P. (2010). Brief: Binary robust independent elementary
339 features. In Daniilidis, K., Maragos, P., and Paragios, N., editors, *Computer Vision – ECCV 2010*,
340 pages 778–792, Berlin, Heidelberg. Springer Berlin Heidelberg.
- 341 Chen, J., Tian, J., Lee, N., Zheng, J., Smith, R. T., and Laine, A. F. (2010). A partial intensity invariant
342 feature descriptor for multimodal retinal image registration. *IEEE Transactions on Biomedical
343 Engineering*, 57(7):1707–1718.
- 344 Collier, O. (2012). Minimax hypothesis testing for curve registration. In Lawrence, N. D. and
345 Girolami, M. A., editors, *Proceedings of the Fifteenth International Conference on Artificial
346 Intelligence and Statistics, AISTATS 2012, La Palma, Canary Islands, Spain, April 21-23, 2012*,
347 volume 22 of *JMLR Proceedings*, pages 236–245. JMLR.org.
- 348 Collier, O. and Dalalyan, A. S. (2013). Permutation estimation and minimax rates of identifiability.
349 *Journal of Machine Learning Research*, W & CP 31 (AI-STATS 2013):10–19.
- 350 Collier, O. and Dalalyan, A. S. (2016). Minimax rates in permutation estimation for feature matching.
351 *The Journal of Machine Learning Research*, 17(1):162–192.
- 352 Comminges, L. and Dalalyan, A. S. (2012). Tight conditions for consistency of variable selection in
353 the context of high dimensionality. *Ann. Stat.*, 40(5):2667–2696.
- 354 Duff, I. S. and Koster, J. (2001). On algorithms for permuting large entries to the diagonal of a sparse
355 matrix. *SIAM Journal on Matrix Analysis and Applications*, 22(4):973–996.
- 356 Flammarion, N., Mao, C., and Rigollet, P. (2019). Optimal rates of statistical seriation. *Bernoulli*,
357 25(1):623–653.
- 358 Gao, C. and Zhang, A. Y. (2019). Iterative algorithm for discrete structure recovery. *arXiv preprint
359 arXiv:1911.01018*.
- 360 Harwood, B. and Drummond, T. (2016). Fanng: Fast approximate nearest neighbour graphs. In *2016
361 IEEE Conference on Computer Vision and Pattern Recognition (CVPR)*, pages 5713–5722.
- 362 Ingster, Y. I. (1982). Minimax nonparametric detection of signals in white Gaussian noise. *Probl. Inf.
363 Transm.*, 18:130–140.
- 364 Ingster, Y. I. and Suslina, I. A. (2003). *Nonparametric goodness-of-fit testing under Gaussian models*,
365 volume 169 of *Lecture Notes in Statistics*. Springer-Verlag, New York.
- 366 Itseez (2015). Open source computer vision library. <https://github.com/itseez/opencv>.
- 367 Jiang, Z., Xie, L., Deng, X., Xu, W., and Wang, J. (2016). Fast nearest neighbor search in the hamming
368 space. In Tian, Q., Sebe, N., Qi, G.-J., Huet, B., Hong, R., and Liu, X., editors, *MultiMedia
369 Modeling*, pages 325–336, Cham. Springer International Publishing.
- 370 Jin, Y., Mishkin, D., Mishchuk, A., Matas, J., Fua, P., Yi, K. M., and Trulls, E. (2020). Image
371 Matching across Wide Baselines: From Paper to Practice. *International Journal of Computer
372 Vision*.

- 373 Juditsky, A. and Nemirovski, A. (2020). *Statistical inference via convex optimization*. Princeton, NJ:
374 Princeton University Press.
- 375 Kuhn, H. W. (1955). The Hungarian Method for the Assignment Problem. *Naval Research Logistics*
376 *Quarterly*, 2(1–2):83–97.
- 377 Kuhn, H. W. (2010). *The Hungarian Method for the Assignment Problem*, pages 29–47. Springer
378 Berlin Heidelberg, Berlin, Heidelberg.
- 379 Laurent, B. and Massart, P. (2000). Adaptive estimation of a quadratic functional by model selection.
380 *Ann. Statist.*, 28(5):1302–1338.
- 381 Lowe, D. G. (2004). Distinctive image features from scale-invariant keypoints. *International journal*
382 *of computer vision*, 60(2):91–110.
- 383 Ma, J., Jiang, X., Fan, A., Jiang, J., and Yan, J. (2021). Image matching from handcrafted to deep
384 features: A survey. *International Journal of Computer Vision*, 129.
- 385 Ma, R., Tony Cai, T., and Li, H. (2020). Optimal permutation recovery in permuted monotone matrix
386 model. *Journal of the American Statistical Association*, pages 1–15.
- 387 Malkov, Y. A. and Yashunin, D. A. (2020). Efficient and robust approximate nearest neighbor search
388 using hierarchical navigable small world graphs. *IEEE Transactions on Pattern Analysis and*
389 *Machine Intelligence*, 42(4):824–836.
- 390 Mao, C., Pananjady, A., and Wainwright, M. J. (2020). Towards optimal estimation of bivariate
391 isotonic matrices with unknown permutations. *Annals of Statistics*, 48(6):3183–3205.
- 392 Mao, C., Weed, J., and Rigollet, P. (2018). Minimax rates and efficient algorithms for noisy sorting.
393 In *Algorithmic Learning Theory*, pages 821–847. PMLR.
- 394 Munkres, J. (1957). Algorithms for the assignment and transportation problems. *Journal of the*
395 *Society for Industrial and Applied Mathematics*, 5(1):32–38.
- 396 Ndaoud, M. and Tsybakov, A. B. (2020). Optimal variable selection and adaptive noisy compressed
397 sensing. *IEEE Trans. Inf. Theory*, 66(4):2517–2532.
- 398 Pananjady, A. and Samworth, R. J. (2020). Isotonic regression with unknown permutations: Statistics,
399 computation, and adaptation. *arXiv preprint arXiv:2009.02609*.
- 400 Pananjady, A., Wainwright, M. J., and Courtade, T. A. (2017). Linear regression with shuffled data:
401 Statistical and computational limits of permutation recovery. *IEEE Transactions on Information*
402 *Theory*, 64(5):3286–3300.
- 403 Ramdas, A., Isenberg, D., Singh, A., and Wasserman, L. A. (2016). Minimax lower bounds for
404 linear independence testing. In *IEEE International Symposium on Information Theory, ISIT 2016,*
405 *Barcelona, Spain, July 10-15, 2016*, pages 965–969. IEEE.
- 406 Rublee, E., Rabaud, V., Konolige, K., and Bradski, G. (2011). Orb: An efficient alternative to sift or
407 surf. In *2011 International Conference on Computer Vision*, pages 2564–2571.
- 408 Shah, N. B., Balakrishnan, S., and Wainwright, M. J. (2021). A permutation-based model for
409 crowd labeling: Optimal estimation and robustness. *IEEE Transactions on Information Theory*,
410 67(6):4162–4184.
- 411 Slawski, M. and Ben-David, E. (2019). Linear regression with sparsely permuted data. *Electronic*
412 *Journal of Statistics*, 13(1):1–36.
- 413 Tian, Y., Balntas, V., Ng, T., Barroso-Laguna, A., Demiris, Y., and Mikolajczyk, K. (2020). D2d:
414 Keypoint extraction with describe to detect approach. In *Proceedings of the Asian Conference on*
415 *Computer Vision (ACCV)*.

- 416 Virtanen, P., Gommers, R., Oliphant, T. E., Haberland, M., Reddy, T., Cournapeau, D., Burovski, E.,
 417 Peterson, P., Weckesser, W., Bright, J., van der Walt, S. J., Brett, M., Wilson, J., Millman, K. J.,
 418 Mayorov, N., Nelson, A. R. J., Jones, E., Kern, R., Larson, E., Carey, C. J., Polat, İ., Feng, Y.,
 419 Moore, E. W., VanderPlas, J., Laxalde, D., Perktold, J., Cimrman, R., Henriksen, I., Quintero,
 420 E. A., Harris, C. R., Archibald, A. M., Ribeiro, A. H., Pedregosa, F., van Mulbregt, P., and SciPy
 421 1.0 Contributors (2020). SciPy 1.0: Fundamental Algorithms for Scientific Computing in Python.
 422 *Nature Methods*, 17:261–272.
- 423 Wang, K., Zhu, N., Cheng, Y., Li, R., Zhou, T., and Long, X. (2018). Fast feature matching based on
 424 r -nearest k -means searching. *CAAI Transactions on Intelligence Technology*, 3(4):198–207.
- 425 Wang, X. (2011). A fast exact k-nearest neighbors algorithm for high dimensional search using
 426 k-means clustering and triangle inequality. In *The 2011 International Joint Conference on Neural
 427 Networks*, pages 1293–1299.
- 428 Wei, Y., Wainwright, M. J., and Guntuboyina, A. (2019). The geometry of hypothesis testing over
 429 convex cones: Generalized likelihood ratio tests and minimax radii. *The Annals of Statistics*,
 430 47(2):994 – 1024.
- 431 Wolfer, G. and Kontorovich, A. (2020). Minimax testing of identity to a reference ergodic markov
 432 chain. In Chiappa, S. and Calandra, R., editors, *The 23rd International Conference on Artificial
 433 Intelligence and Statistics, AISTATS 2020, 26-28 August 2020, Online [Palermo, Sicily, Italy]*,
 434 volume 108 of *Proceedings of Machine Learning Research*, pages 191–201. PMLR.
- 435 Xing, X., Liu, M., Ma, P., and Zhong, W. (2020). Minimax nonparametric parallelism test. *Journal
 436 of Machine Learning Research*, 21(94):1–47.

437 Checklist

- 438 1. For all authors...
- 439 (a) Do the main claims made in the abstract and introduction accurately reflect the paper’s
 440 contributions and scope? [Yes] See Section 1.
- 441 (b) Did you describe the limitations of your work? [Yes] See Section 1 and Section 2 for
 442 informal statements, precise assumptions/limitations are presented in Section 3.
- 443 (c) Did you discuss any potential negative societal impacts of your work? [N/A]
- 444 (d) Have you read the ethics review guidelines and ensured that your paper conforms to
 445 them? [Yes]
- 446 2. If you are including theoretical results...
- 447 (a) Did you state the full set of assumptions of all theoretical results? [Yes] See Section 3.
- 448 (b) Did you include complete proofs of all theoretical results? [Yes] See supplemental
 449 material (Appendix B).
- 450 3. If you ran experiments...
- 451 (a) Did you include the code, data, and instructions needed to reproduce the main experi-
 452 mental results (either in the supplemental material or as a URL)? [Yes] See supplemen-
 453 tal material.
- 454 (b) Did you specify all the training details (e.g., data splits, hyperparameters, how they
 455 were chosen)? [Yes] See Section 5 and supplemental material (Appendix D).
- 456 (c) Did you report error bars (e.g., with respect to the random seed after running experi-
 457 ments multiple times)? [Yes] See Section 5 and supplemental material (Appendix D).
- 458 (d) Did you include the total amount of compute and the type of resources used (e.g., type
 459 of GPUs, internal cluster, or cloud provider)? [N/A]
- 460 4. If you are using existing assets (e.g., code, data, models) or curating/releasing new assets...
- 461 (a) If your work uses existing assets, did you cite the creators? [Yes]
- 462 (b) Did you mention the license of the assets? [N/A]
- 463 (c) Did you include any new assets either in the supplemental material or as a URL? [N/A]
- 464

- 465 (d) Did you discuss whether and how consent was obtained from people whose data you're
466 using/curating? [N/A]
- 467 (e) Did you discuss whether the data you are using/curating contains personally identifiable
468 information or offensive content? [N/A]
- 469 5. If you used crowdsourcing or conducted research with human subjects...
- 470 (a) Did you include the full text of instructions given to participants and screenshots, if
471 applicable? [N/A]
- 472 (b) Did you describe any potential participant risks, with links to Institutional Review
473 Board (IRB) approvals, if applicable? [N/A]
- 474 (c) Did you include the estimated hourly wage paid to participants and the total amount
475 spent on participant compensation? [N/A]